sustainability

MDPI

Article

Modeling Mushrooms' Carbon Dioxide Emission and Heat Exchange Rates for Synergistic Cultivation with Leafy Greens

Marc-Antoine Meilleur [1,*], Diane Bastien [2] and Danielle Monfet [3]

[1] Department of Mechanical Engineering, École de Technologie Supérieure, Montreal, QC H3C 1K3, Canada
[2] Department of Technology and Innovation, University of Southern Denmark, 5230 Odense M, Denmark; dib@iti.sdu.dk
[3] Department of Construction Engineering, École de Technologie Supérieure, Montreal, QC H3C 1K3, Canada; danielle.monfet@etsmtl.ca
* Correspondence: marc-antoine.meilleur.1@ens.etsmtl.ca

Abstract: The cultivation of mushrooms in controlled environments generates a significant amount of CO_2 as a by-product. This presents opportunities for carbon dioxide (CO_2) enrichment in leafy green production. This study aimed to develop a model for CO_2 emission and heat exchange rates that can be used to support the synergistic cultivation of mushrooms and leafy greens. This was achieved by aggregating data from literature with experimental data gathered in two different testing spaces. The average CO_2 emission and heat exchange rates for shiitake incubated at 21 °C were determined and a CO_2 emission rate model for mixed substrate in incubation was developed based on indoor temperature variations. The results indicated that oyster mushrooms have a notable CO_2 enrichment potential, twice that of shiitake in the incubation stage and five times more in fructification. Additionally, oyster mushrooms released a significant amount of heat during incubation. In contrast, shiitake mushrooms with their minimal heat exchange rate during incubation could offer an energy-efficient option for synergistic cultivation with leafy greens in environments where cooling is required year-round. Moreover, it was observed that the CO_2 emission rate of a full-scale incubation chamber is strongly correlated with indoor temperature. These findings offer valuable information for modeling the CO_2 emission and heat exchange rates of mushroom and leafy green farms.

Keywords: mushroom CO_2 emission rate; mushroom heat exchange; CO_2 enrichment; circular economy; sustainable agriculture

check for updates

Citation: Meilleur, M.-A.; Bastien, D.; Monfet, D. Modeling Mushrooms' Carbon Dioxide Emission and Heat Exchange Rates for Synergistic Cultivation with Leafy Greens. *Sustainability* **2023**, *15*, 16740. https://doi.org/10.3390/su152416740

Academic Editors: Marie-Jose Montpetit and Nicolas Merveille

Received: 25 October 2023
Revised: 4 December 2023
Accepted: 5 December 2023
Published: 11 December 2023

Copyright: © 2023 by the authors. Licensee MDPI, Basel, Switzerland. This article is an open access article distributed under the terms and conditions of the Creative Commons Attribution (CC BY) license (https://creativecommons.org/licenses/by/4.0/).

1. Introduction

The cultivation of mushrooms can be traced back to as early as 600 BC, starting with wood ear mushrooms (*Auricularia auricula*), cultivated on logs in China. Around 60 strains are commercially grown, with a select 10 produced on an industrial scale [1]. The 1980s was a pivotal period marked by the introduction of indoor cultivation in controlled environments, which led to a significant rise in global mushroom production [2]. Recent advancements indicate that interconnected smart farms represent the next frontier for optimizing these cultivation spaces [3,4]. Such interconnectivity enables real-time data exchange, thus allowing the integration of various agricultural processes to attain ecological and economic targets [5,6].

As such, there is untapped potential to implement solutions enabling the circular economy. One example of this concept is the cultivation of mushrooms and leafy greens in controlled environment agriculture (CEA). This combination can be synergistic, as the CO_2 emitted by mushrooms through respiration becomes a valuable resource for improving the growth environment of leafy greens, thereby enhancing photosynthesis [7,8]. This synergy warrants consideration, as CO_2 enrichment typically stems from non-environmentally friendly fossil fuel combustion or costly pure liquefied CO_2 [9].

Enriching the leafy green environment with CO_2 released from mushroom growth has been studied in controlled environment experiments on bench tests with shiitake [10] and king oyster [7,11] strains combined with lettuces. These studies consistently demonstrated the feasibility of CO_2 exchange between the two crops. Still, the results were limited to the fructification growth stage of mushrooms, leaving the incubation stage, which represents about one-third of the life cycle production of mushrooms [12], unexplored.

Leafy greens grown in CEA with artificial lighting generate heat, often necessitating year-round cooling [13]. Similarly, mushroom substrates in CEA are exothermic [12,14,15]. However, all studies on the synergies between mushrooms and leafy greens have overlooked the thermal interactions between the two crops. This oversight is significant, as heat exchanges between these crops can critically impact the energy efficiency of a synergistic system. Factors such as crop strains, temperature and humidity setpoints, lighting, and local climate play a role. Integrating both CO_2 emission and heat exchange rates as part of the analysis would offer a more realistic picture of the benefits of this synergy, as illustrated in Figure 1.

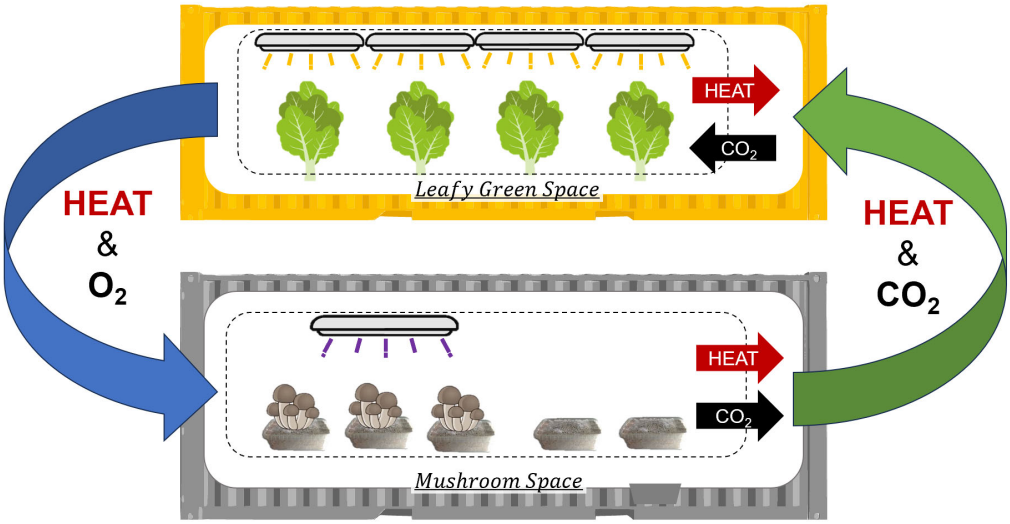

Figure 1. Conceptual diagram of mushrooms and leafy greens synergistic cultivation.

To develop a comprehensive CO_2 and energy exchange model between mushrooms and leafy greens, specific data on CO_2 emission and heat exchange rates for shiitake and oyster mushrooms are essential but currently lacking. Notably, mushrooms generate significant heat during the incubation stage due to thermogenesis [14]. Koncsag & Kirwan [15] quantified the heat exchange rate for oyster mushrooms during this stage, but such data are missing for shiitake. Despite the interest in mushroom cultivation, there are few quantitative analyses on their CO_2 emission rates [15]. In the 1970s, a theoretical model describing mycelium growth and CO_2 emission rate was developed based on the dried mass of mycelium and mushroom fruit [16]. Recently, Jung & Son [17] introduced an empirical model adapted from one proposed by Chanter & Thornley, which predicts the CO_2 emission rates of king oyster mushrooms during the fructification stage considering indoor temperature and time. The results indicated that CO_2 emission rates increased exponentially with time and linearly with temperature. However, the CO_2 model was limited to king oyster mushrooms, no model was proposed for the incubation stage, and no information related to the heat exchange rate was documented. No CO_2 emission rate models appear to exist for shiitake, but a study has been conducted across various shiitake strains that reported the CO_2 emitted for both the incubation and fructification stages at 24 °C [18]. Unlike oyster mushrooms, shiitake mushrooms are generally grown at lower temperatures, such as 21 °C [12]. Opting for a production temperature of 21 °C could prove more advantageous for synergistic cultivation with leafy greens, as it would result in lower cooling loads for the leafy greens when grown in a controlled environment [13].

Moreover, developing a model that provides the CO_2 exchange rate of a typical full-scale incubation chamber housing a variety of mushroom genera and strains at diverse growth stages would offer valuable complementary data to small-scale experiments, as is often the case in commercial mushroom farms [12].

The experimental results aim to advance sustainability in mushroom cultivation by investigating CO_2 emission and heat exchange rates, specifically focusing on oyster and shiitake mushrooms and their interaction with leafy greens. They provide valuable data on the CO_2 emission and thermal exchange rates of shiitake mushrooms at lower indoor temperatures, addressing gaps in the existing literature. The study also evaluates CO_2 emission rates in mixed-genus incubation chambers, developing a temperature-based emission model. These insights are crucial for developing global CO_2 emission and energy model for mushroom and leafy green, representing the next step of quantifying the benefits of synergetic cultivation between these two crops.

2. Materials and Methods

This study is based on experiments in two distinct testing spaces: (1) a controlled small-scale test bench and (2) a full-scale incubation chamber of a mushroom farm. These spaces were used to conduct three experiments to develop an empirical mass and energy balance model for mushrooms. This section provides an overview of the testing spaces, outlines the experimental setup, and details the model's development and validation process. The equations used to convert CO_2 emission data from existing literature into useful metrics for comparison with the experimental results are also introduced.

2.1. Average CO_2 Emission Rates

In commercial mushroom cultivation, a common practice is to adopt staggered production or diversified growing techniques to maintain a steady harvest. This requires carefully timing the inoculation, incubation, and fructification stages across different mushroom batches, ensuring a continuous harvesting cycle. As a result, there is a mix of growth stages at any given time on the farm. An average CO_2 emission rate for both the incubation stage and fructification stage is used to assess this strategy. The current literature on CO_2 emission rates within the mushroom growth cycle is limited. Existing studies have either aggregated the CO_2 emission rates over time, as shown in Table 1, or have developed CO_2 emission rates using predicting models at specific times using Equations (1) and (2).

Table 1. CO_2 emissions for a specific growth stage and strain available in the literature.

Genus	Growing Stage	Strain [1]	Cumulative Sum [g CO_2]	Substrate Mass [kg]	Period [Days]	Setpoints	Substrate Mix Ratio
Pearl Oyster (*Pleurotus ostreatus*) [8]	Incubation	n/a	120	1.36	14	20–25 °C	mesquite:alfalfa | 1:1
		n/a	55	1.36	14		straw:cotton | 3:1
		n/a	88	1.36	14		oak:soy | 1:1
Shiitake (*Lentinula edodes*) [18]	Incubation	931	132	1	50	24 °C, 80% HR	wood chip:wheat bran | 4:1
		HuxiangF2	156	1	50		
		Qihe7	146	1	50		
		Shengxiang215	155	1	50		
	Fructification	931	74	1	23		
		HuxiangF2	85	1	40		
		Qihe7	83	1	40		
		Shengxiang215	114	1	90		

[1] n/a stands for not available.

$$\dot{R}_b = \left(9.670{\cdot}10^{-5}{\cdot}T^2 - 5.062{\cdot}10^{-3}{\cdot}T + 0.0789\right){\cdot}e^{0.549{\cdot}DAS} - 1.313{\cdot}10^{-5}{\cdot}T^2 + 2.412{\cdot}T + 0.117 \quad (1)$$

$$\dot{R}_a = \left(9.670{\cdot}10^{-5}{\cdot}T^2 - 4.363{\cdot}10^{-4}{\cdot}T + 8.089{\cdot}10^{-3}\right){\cdot}e^{0.549{\cdot}DAS} + 0.027{\cdot}T^2 + 5.108{\cdot}T - 30.732 \quad (2)$$

Here, $\dot{R}_b$ and $\dot{R}_a$ are the CO_2 emission rate of 0.57 kg of king oyster substrate in the fructification stage before and after tinning, respectively [μg $CO_2{\cdot}s^{-1}{\cdot}$], T is the indoor air temperature [°C], and DAS is the number of days since the start of the fructification stage. In the model, Equation (1) was used from DAS 1 to 12, and Equation (2) was used from DAS 12 to 17 [19].

In studies that present cumulative CO_2 emission rates over a specific growth cycle and period, the average CO_2 emission rate was calculated by dividing the total emitted CO_2 by the duration of the experiment and substrate mass, as described in Equation (3):

$$\dot{R}_{avg} = \frac{R_p}{t_p{\cdot}m_{sub}} \quad (3)$$

Here $\dot{R}_{avg}$ is the average CO_2 emission rate of substrate [μg $CO_2{\cdot}s^{-1}{\cdot}kg_{sub}{}^{-1}$], R_p is the mass of CO_2 emitted during the specific period [μg CO_2], t_p is the duration of the experiment [s], and m_{sub} is the substrate mass [kg].

To determine the average CO_2 emission rate using Equations (1) and (2), the average CO_2 emission rate at a specific indoor temperature throughout the entire cycle was calculated using Equation (4), where DCB and DCA represent the days of the cycle before and after thinning, respectively.

$$\dot{R}_{avg} = \frac{\sum_{DAS=1}^{DCB}\dot{R}_b(T,\ DAS) + \sum_{DAS=12}^{DCA}\dot{R}_a(T,\ DAS)}{(DCB + DCA){\cdot}m_{sub}} \quad (4)$$

2.2. Description of the Testing Spaces

The following section presents an in-depth overview of the two testing spaces used in the study: the small-scale (SS) test bench and the full-scale (FS) incubation chamber. The section details the specifications and equipment of these spaces. These spaces were equipped with data acquisition systems for monitoring the indoor environmental conditions, as described in Table 2.

Table 2. Details of the data acquisition installed in the spaces.

Space Type	Sensor Type	Brand	Accuracy	Location
Small-scale (SS) test bench	Temperature (t) [°C] and relative humidity (hum) [%]	J&J HE-67N2-0N00P	±0.6 °C ±3% RH	Supply Air, Return Air, Indoor Air
	CO_2 concentration (CO2) [ppm]	Honeywell IAQPOINT2	±30 ppm +3%	Supply Air, Return Air, Indoor Air
	Airspeed (V_{air}) [$m{\cdot}s^{-1}$]	Ebtron EF-A1121-T-12	±3%	Return Air
Full-scale (FS) incubation chamber	Temperature (t) [°C] and relative humidity (hum) [%]	Sensirion SHT31	±0.3 °C ±2% RH	Supply Air, Return-Air
	CO_2 concentration (CO2) [ppm]	Telaire T6713-5K	±30 ppm ±3%	Return Air
		SenseAir S8	±3%	Supply Air
	Airspeed (V_{air}) [$m{\cdot}s^{-1}$]	Modern Device RevP	±10%	Return Air

2.2.1. Small-Scale (SS) Test Bench

The small-scale test bench is a 3.02 m × 2.44 m × 1.97 m (volume of 14.5 m^3) space located within a building maintained at an indoor temperature of approximately

20–21 °C (Figure 2a). The walls, floor, and ceiling of the test bench were constructed from polyurethane-insulated panels with an overall U-value of 0.12 $W \cdot (K \cdot m^2)^{-1}$, a thermal capacity of 1000 $J \cdot (kg \cdot K)^{-1}$, and a density of 113.17 $kg \cdot m^{-3}$. The surfaces were covered with plastic water-repellent panels to prevent water vapor diffusion, with an airtightness of 3.7 ACH @ 50 Pa. The conditions inside the small-scale test bench were controlled using heating, ventilation, and air conditioning (HVAC) equipment, with a return air duct area (A_{duct}) of 0.124 m^2. The sensor locations in the test bench are illustrated in Figure 2b. Two different air loop configurations are possible: an open-loop (OL) and closed-loop (CL). For the closed-loop (CL) configuration, the HVAC equipment was turned off, allowing the indoor conditions (temperature, humidity, and CO_2 concentration) to increase inside the chamber, enabling the use of differential equations to estimate the CO_2 emission and heat exchange rates.

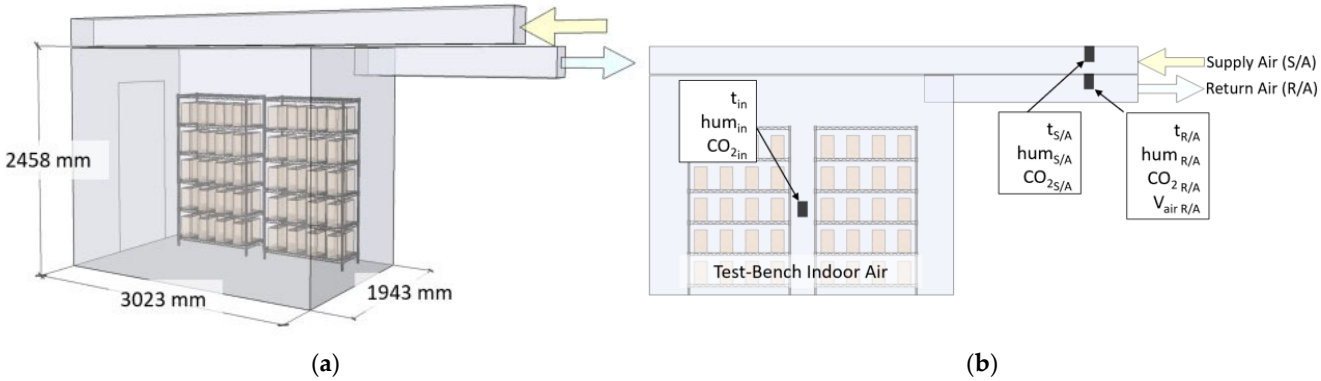

Figure 2. Small-scale test bench: (**a**) 3D view and (**b**) location of sensors.

2.2.2. Full-Scale (FS) Incubation Chamber

The full-scale incubation chamber of a mushroom farm located in Quebec, Canada (Figure 3a) was used as a second testing space. The incubation chamber has a volume of 56 m^3, where the indoor air temperature and CO_2 concentration are regulated by an HVAC system, which has a return air duct (A_{duct}) with an area of 0.025 m^2.

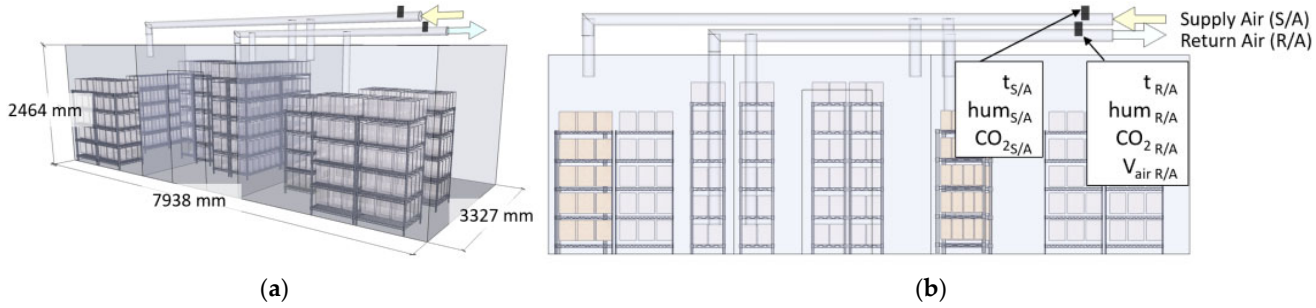

Figure 3. Full-scale (FS) incubation chamber: (**a**) 3D view and (**b**) location of sensors.

The test bench has an Arduino Mega microcontroller data acquisition system connected to the farm's Ethernet network. Temperature, humidity, and CO_2 concentration readings of the supply air and return air of the incubation chambers were recorded as illustrated in Figure 3b and detailed in Table 2. Only an open-loop (OL) configuration is possible in this space.

2.3. Description of the Experiments

For all experiments, each substrate bag consisted of the following mass proportions: 70% wood sawdust, 20% bran, 10% mycelium on grain and water to saturation, with an average weight of 3 kg per bag. During incubation, bags were kept at indoor temperatures

of 18–24 °C, CO_2 concentrations of 800–1000 ppm, and without relative humidity control. For each experiment, the colonization ratio was about 50%, representing the real-life operation of an incubation chamber. The substrate colonization ratio is the fraction of substrate bags that are fully colonized, i.e., the incubation stage is completed and the substrate is ready to be transferred to the fructification stage. A substrate bag is determined to be fully colonized by visual inspection when the outer surface of the substrate was totally white. The two testing spaces were used to conduct three distinct experiments, all in the incubation stage of mushroom production: SS-OL-53%, SS-CL-53%, and FS-OL-44%, as described below.

SS-OL-53%: This experiment determined the average CO_2 emission rate of Shiitake mushrooms incubating at an indoor temperature of 21 °C. This was achieved using an open-loop (OL) ventilation configuration where the supply ($CO2_{S/A}$) and return air ($CO2_{R/A}$) CO_2 concentrations were measured as well as the return air speed ($V_{air}R/A$). Data were collected every minute and averaged over 30 min for 14 h. During this experiment, there is 215 kg of shiitake substrate, 53% of which is fully colonized.

SS-CL-53%: This experiment was used to evaluate the heat exchange rate of Shiitake substrate in incubation and to validate the CO_2 emission rate results of experiment SS-OL-53%. This was achieved using a closed-loop (CL) ventilation configuration, i.e., no forced airflow, and all air dampers were closed. Thus, the CO_2 and heat rise over time in the CL configuration. Data were analyzed when steady-state conditions were attained and stopped when either the CO_2 concentration ($CO2_{S/A}$) reached 2000 ppm (probe saturation value) or the indoor temperature ($temp_{in}$) reached 24 °C. Except for the ventilation configuration, this setup was identical to SS-OL-53%, a small-scale test bench with 215 kg of 53% colonized shiitake substrate.

FS-OL-44%: This experiment was conducted in a full-scale incubation chamber with mixed substrate strains and aims to develop a CO_2 emission rate model based on the indoor temperature. This was achieved using an open-loop (OL) ventilation configuration. The difference in CO_2 concentration between the supply ($CO2_{S/A}$) and return air ($CO2_{R/A}$) was used to complete the emission rate calculations. Data were recorded every 5 min and averaged over an hour for 75 h. Data recorded during and for an hour following the presence of workers in the chamber were excluded. During this experiment, there was 1827 kg of mixed substrate (46% shiitake, 44% oyster, 10% lion's mane), with 44% fully colonized.

2.4. Experimental Model Development

The equations presented in this section quantify the CO_2 emission and heat exchange rates based on the experimental data.

2.4.1. CO_2 Emission Rate

The CO_2 emission rate, which indicates the respiratory activity of the mushroom substrate, is calculated using approaches derived from indoor air quality science [20]. A conversion factor k [7] is included to fit with experimental conditions. For the open-loop (OL) experiments, the steady-state CO_2 balance between the return and supply air in the chamber was estimated using Equation (5). For the closed-loop (CL) experiment, SS-CL-53%, a differential equation comparing the CO_2 concentration at the beginning and end of the experiment was used instead, as described by Equation (6).

$$\dot{R} = \frac{(C_{out} - C_{in}) \cdot k \cdot V_{air} \cdot A_{duct}}{m_{sub}} \quad (5)$$

Here, $\dot{R}$ is the CO_2 emission rate of substrate [μg $CO_2 \cdot s^{-1} \cdot kg_{sub}{}^{-1}$], C_{in} and C_{out} are the CO_2 concentration of supply air (S/A) and return air (R/A) from the test bench, respectively [μmol·mol^{-1}], k equals to 1830 and is a unit conversion factor from CO_2 μmol·mol^{-1} to μg

$CO_2 \cdot m^{-3}$ at 20 °C, V_{air} is the return air speed [$m \cdot s^{-1}$], A_{duct} is the return duct area [m^2], and m_{sub} is the substrate mass [kg].

$$\dot{R} = \frac{dR}{dt} = \frac{(C_e - C_b) \cdot k \cdot V \cdot 10^3}{(t_e - t_b) \cdot m_{sub}} \quad (6)$$

Here, R is the mass of CO_2 in the test bench [$\mu g\ CO_2 \cdot kg_{sub}{}^{-1}$], t is the time [s], C_b and C_e are the CO_2 concentration at the beginning and the end of the experiment, respectively [$\mu mol \cdot mol^{-1}$], V is the test bench volume [m^3], and t_b and t_e are the time at the beginning and the end of the experiment, respectively [s].

Since the full-scale (FS) test bench FS-OL-44% is an existing incubation chamber of a mushroom farm with an average weekly production of 560 kg, it experienced fluctuations in indoor air temperature. Considering that the CO_2 emission rate of mycelium increases linearly according to temperature [17], linear regression was used to represent the relationship between CO_2 emission rate, return air temperature, and substrate mass (Equation (7)). To ensure unbiased results, all measurement time stamps were randomly shuffled using the Mersenne Twister algorithm [21]. The regression was constructed using the first two-thirds of the data points, while the last third was used to validate the accuracy of the regression, as follows:

$$\dot{R} = \left(a_1 \cdot T_{out} + a_2\right) \cdot m_{sub} \quad (7)$$

Here, T_{out} is the return temperature of the test bench [°C], and $a_{1,}$ a_2 are regression coefficients [dimensionless].

2.4.2. Heat Exchange Rate

The heat exchange rate quantifies the rate of thermal energy transfer between the mushroom substrate and its environment. This is estimated using equations typically used to describe HVAC systems [20]. The heat exchange rate was calculated solely for the small-scale (SS) experiments. It was estimated using differential Equation (8), which calculates the difference in enthalpy at the test beginning and ending.

$$\dot{Q} = \frac{dh}{dt} \cdot V \cdot \rho_{da} = \left(\frac{h_e - h_b}{t_e - t_b}\right) \cdot V \cdot \rho_{da} \cdot 10^3 \quad (8)$$

Here, $\dot{Q}$ is the heat exchange rate from the mushroom substrate [W], h is the specific enthalpy [$kJ \cdot kg_{da}{}^{-1}$], ρ_{da} equals 1.19 and is the average air density during the experiment [$kg \cdot m^{-3}$], and h_b and h_e are the specific enthalpies at the beginning and at the end of the experiment, respectively, estimated using Equation (9).

$$h = h_{da} + W \cdot h_g \quad (9)$$

Here, h_{da} is the specific enthalpy of dry air [$kJ \cdot kg_{da}{}^{-1}$], h_g is the specific enthalpy for saturated water vapor [$kJ \cdot kg_{da}{}^{-1}$], and W is the humidity ratio [$kg_w \cdot kg_{da}{}^{-1}$]. The humidity ratio is computed using Equation (10), as follows:

$$W = 0.622 \cdot \frac{hum \cdot P_{ws}}{P - hum \cdot P_{ws}} \quad (10)$$

Here, hum is the relative humidity expressed as a fraction, P_{ws} is the saturation pressure [Pa], and P is the atmospheric pressure [Pa]. The saturation pressure over liquid water is given by Equation (11) and C_1 to C_6 are listed in Table 3.

$$\mathrm{Ln}\ P_{ws} = \frac{C_1}{T^*} + C_2 + C_3 T + C_4 T^2 + C_5 T^3 + C_6 \mathrm{Ln}\ T \quad (11)$$

Here, T^* is the absolute temperature [$t + 273.15$].

Table 3. Coefficients C1 to C6 [20].

C_1	C_2	C_3	C_4	C_5	C_6
-5.800×10^3	1.391×10	-4.864×10^{-2}	4.176×10^{-5}	-1.445×10^{-8}	6.546×10

2.4.3. Full-Scale Experimental Model Validation

The data collected during the FS experiment FS-OL-44% were divided into two subsets: the first two-thirds were used to create the regression, while the last third was used to validate the regression model. The regression was checked using the *p*-value and R^2. A *p*-value less than 0.05 indicates a satisfactory level of confidence, and the closer R^2 is to 1, the more the variance in the CO_2 emission rate is explained by the variation of the indoor air temperature. Also, the mean relative deviation (MRD), defined according to Equation (12), was used to assess the accuracy between the measured data and the estimated CO_2 emission rate using the proposed model [22]. A lower MRD indicates that the model's predictions closely match the measured values. A MRD of less than 10% signifies a strong correlation, while a MRD within the 10–20% range represents average accuracy. Conversely, a MRD exceeding 20–30% is deemed insufficient.

$$MRD = \left[\frac{100}{N} \sum_{i=1}^{n} \frac{(R_{mes} - R_{est})}{R_{mes}} \right] \quad (12)$$

Here, MRD is the mean relative deviation, N is the sample size, R_{mes} are the measured data from the validation sample, and R_{est} are the values estimated from the model.

3. Results

The CO_2 emission rate was estimated using data gathered from the SS and FS testing spaces, while the heat exchange rate solely used data collected from the SS test bench. These results were then aggregated with data from the literature, as detailed in Table 1, to propose a comprehensive summary of CO_2 emission and heat exchange rates.

3.1. CO_2 Emission Rate from Small-Scale (SS) Experiments

The CO_2 emission rate was computed using Equation (5) and remains relatively constant throughout the small-scale (SS) experiment, as depicted in Figure 4. The average CO_2 emission rate for the incubation of shiitake substrate, SS-OL-53%, is 24.9 ± 16.6 µg $CO_2 \cdot s^{-1} \cdot kg_{sub}^{-1}$ with a standard deviation of 0.9 µg $CO_2 \cdot s^{-1} \cdot kg_{sub}^{-1}$.

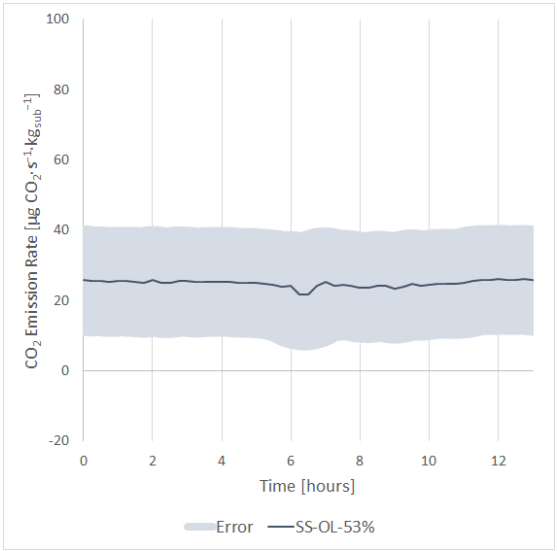

Figure 4. CO_2 emission rate of incubating shiitake substrate during the SS-OL-53% experiment.

As described in Section 3.3, the closed-loop (CL) experiment SS-CL-55% was conducted to validate the results obtained from the SS-OL-53% using Equation (6). The experiment started with a CO_2 concentration of 534 ppm (14.3 g of CO_2) and reached probe saturation at 2000 ppm (53.5 g of CO_2) after 100 min. Data from the first 10 min were omitted from the analysis to account for steady-state conditions to be reached. A solid linear regression, with an R^2 value of 0.99, was found between the 10th and 90th minutes, as shown in Figure 5, yielding an average CO_2 emission rate of 30.9 ± 3.8 μg $CO_2 \cdot s^{-1} \cdot kg_{sub}^{-1}$, which aligns with the findings from the open-loop (OL) experiment.

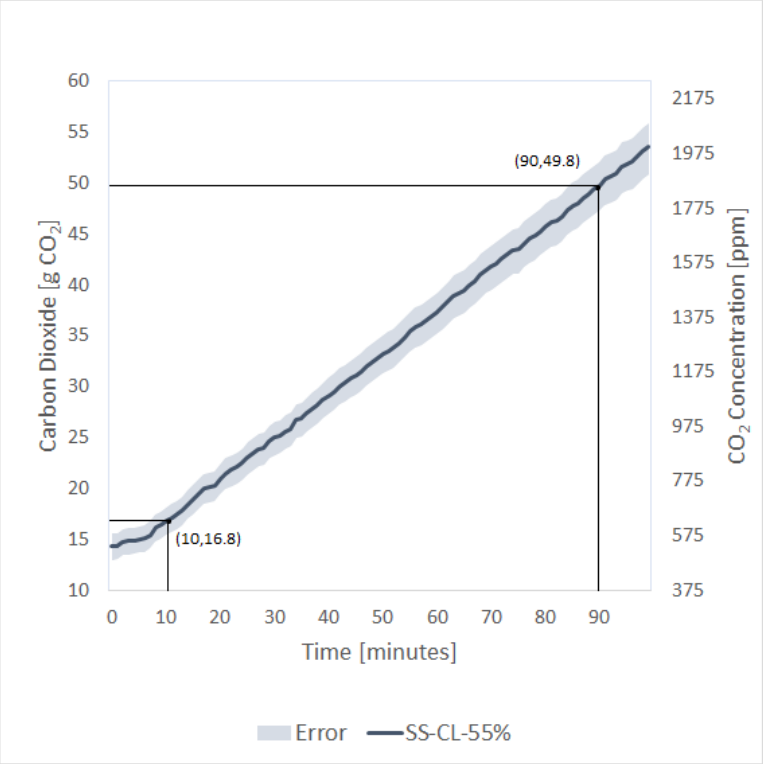

Figure 5. Accumulation of CO_2 from incubation of shiitake substrate during SS-CL-55% experiment.

3.2. CO_2 Emission Rate from Full-Scale (SS) Experiment

Using the data gathered from the FS testing spaces, the regression model depicted in Figure 6 is established, exhibiting an R^2 value of 0.88, indicating a strong correlation. The regression coefficients, a_1 and a_2, are 1.99 ± 0.11 and −4.09 ± 1.02, respectively, with a p-value of 0.049. Thus, Equation (7) can be rewritten as Equation (13) to model the CO_2 emission rate of mixed substrate.

$$\dot{R} = (1.99 \cdot T_{R/A} - 4.09) \cdot m_{sub} \quad (13)$$

As demonstrated in Figure 7, the R^2 value of 0.90 signifies a good fit of the model to the data. Concurrently, the MRD—a measure of proximity between estimated and measured values described by Equation (12)—indicates an average absolute discrepancy of a mere 3.7%. This relatively low MRD highlights the predictive performance of the model.

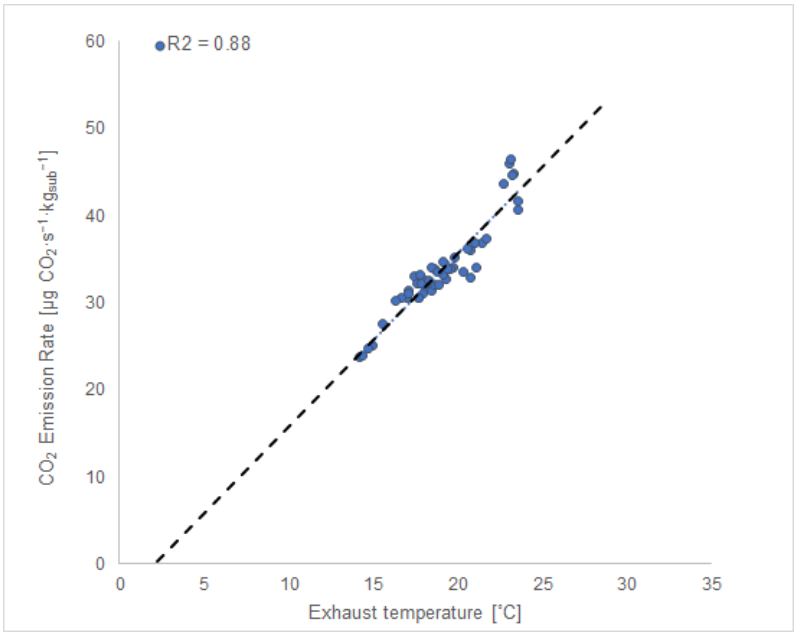

Figure 6. Changes in the CO_2 emission rate per kg of mixed mushroom substrate in response to variation in return air temperature during the FS-OL-44% experiment.

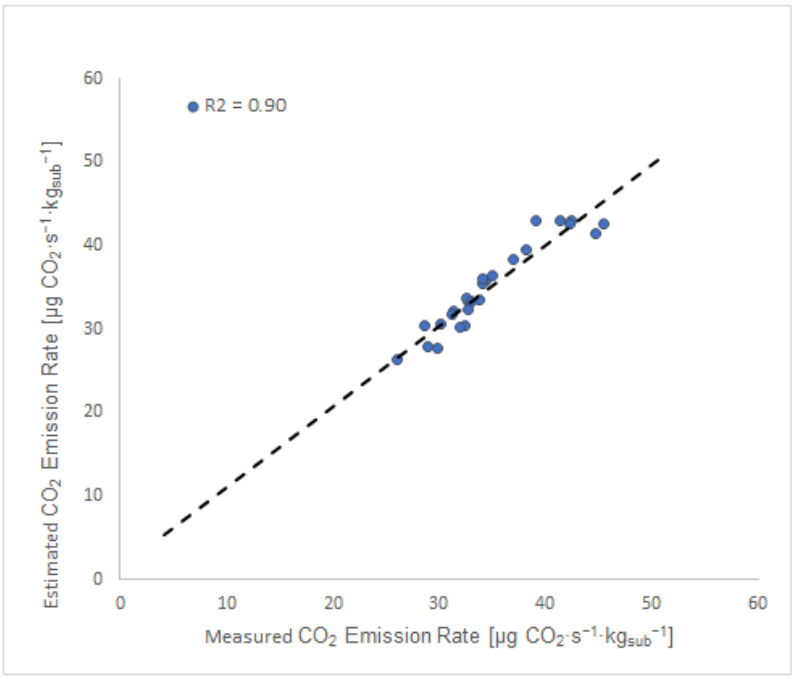

Figure 7. Comparison between the measured and estimated CO_2 emission rate of mixed mushroom substrate.

3.3. Heat Exchange Rate from Small-Scale (SS) Experiment

The sensible and latent heat exchange rate, estimated using Equation (4) with data from the small-scale SS-CL-53% experiment, revealed minimal heat released from the substrate, averaging 4.2 ± 3.0 W for the bench test containing 215 kg of shiitake substrate. Nonetheless, it is essential to acknowledge that a heat exchange does occur, as indicated by the steady rise in indoor air temperature and relative humidity, as presented in Table 4. Figure 8 illustrates a gradual increase in the enthalpy of the test bench, starting around the 60-min mark. This is further supported by the strong linear correlation, with an R^2 value of

0.99, observed between the 60th and 360th minutes. These observations suggest a minor release of sensible and latent heat within the system.

Table 4. Indoor air conditions during the SS-CL-53% experiment.

Time [Minutes]	0	60	360
Indoor air temperature [°C]	22.3	23.0	24.0
Indoor air relative humidity [%]	26.8	28.9	34.4
Indoor air enthalpy [kJ]	588.2	623.0	698.3

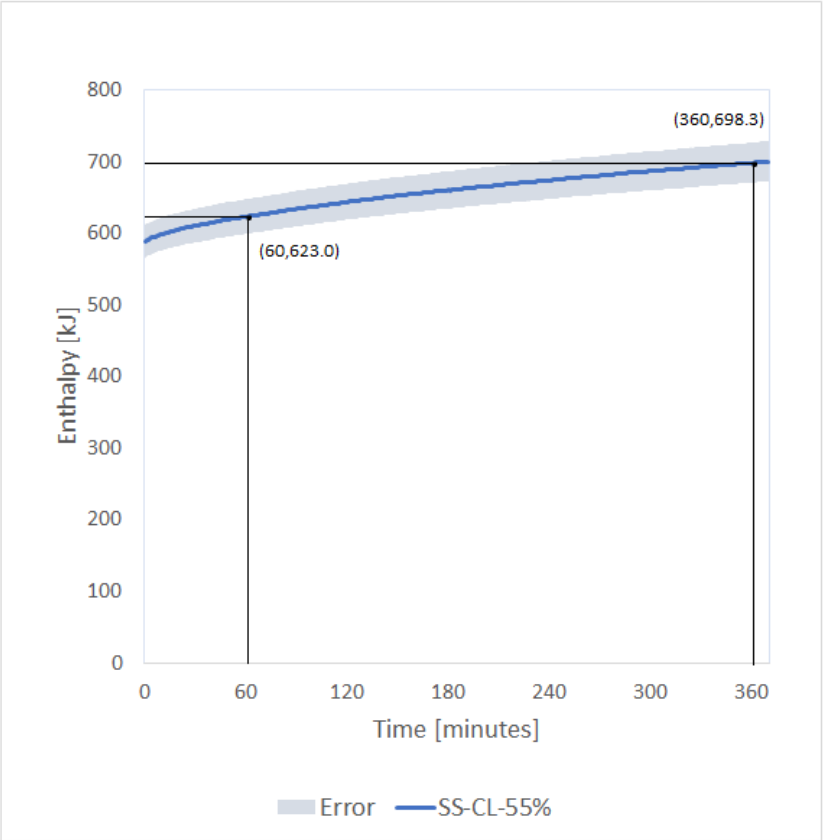

Figure 8. Increase enthalpy from incubating shiitake substrate during closed-loop (CL) SS-CL-55% experiment.

3.4. Aggregated CO_2 Emission and Heat Exchange Rates

To support the analysis of potential synergies between mushrooms and leafy greens production, data from the literature described in Section 3.1 were supplemented with the experimental results presented in Sections 4.1 and 4.2. As such, Table 5 aggregates and summarizes the CO_2 emission rates for oyster and shiitake mushrooms during their incubation and fructification stages. In contrast, Table 6 presents the heat exchange rate for the oyster and shiitake mushrooms.

Table 5. Average CO_2 emission rates of mushrooms.

Genus	Growing Stage	Strain	Average CO_2 Emission Rate [$\mu gCO_2 \cdot s^{-1} \cdot kg_{sub}^{-1}$]	Setpoints [1]	Reference
Oyster	Incubation [5]	n/a [6]	53.5	20–25 °C	Hyunja Chung [8]
	Fructification [2]	King Oyster	108.8 @ 18 °C 129.1 @ 21 °C 150.8 @ 24 °C	16–25 °C 85% HR	Jung & Son [17]
Shiitake	Incubation	n/a	24.9	21 °C	SS-OL-53% experimental results
		931	32.8	24 °C	Ou et al. [18]
		HuxiangF2	38.3		
		Qihe7	35.8		
		Shengxiang215	35.5		
		Average	35.6		
	Fructification	931	37.4	24 °C 80% HR	
		HuxiangF2	24.9		
		Qihe7	24.4		
		Shengxiang215	19.9		
		Average	26.7		
Mixed [4]	Incubation [3]	n/a	31.7 @ 18 °C 37.7 @ 21 °C 43.7 @ 24 °C	15–25 °C	FS-OL-44% experimental results

[1] "–" indicates the temperature range of the experiment; [2] extracted for specific temperatures (18, 21, 24 °C) using Equation (4); [3] extracted for specific temperatures (18, 21, 24 °C) using Equation (13); [4] 46% shiitake, 44% oyster and 10% lion's mane; [5] only the value for the oak substrate is presented; [6] n/a stands for not available.

Table 6. Heat exchange rates of mushrooms.

Genus	Growing Stage	Heat Exchange Rate [$W \cdot kg_{sub}^{-1}$]	Substrate	Reference
Oyster	Incubation	7.08	Wheat straw	Koncsag & Kirwan [15]
Shiitake	Incubation	0.02	Wood chips	SS-CL-53% experimental results

4. Discussion

These experiments offer valuable insights into CO_2 emission and heat exchange rates from the mushroom substrate in incubation under controlled environments.

4.1. CO_2 Emission Rate

In the small-scale experiments, the mushroom substrate demonstrated a relatively stable CO_2 emission rates during the open-loop experiment SS-CL-53% (24.9 ± 16.6 μg $CO_2 \cdot s^{-1} \cdot kg_{sub}^{-1}$), which are corroborated by the closed-loop experiment SS-CL-53% (30.9 ± 3.8 μg $CO_2 \cdot s^{-1} \cdot kg_{sub}^{-1}$). A prior study by Ou et al. [18] revealed slightly elevated average CO_2 emission rates, ranging from 32.8 to 38.3 μg $CO_2 \cdot s^{-1} \cdot kg_{sub}^{-1}$ across four distinct Shiitake strains. This disparity is likely attributable to the experimental indoor air temperature set at 21 °C, which contrasts with the 24 °C used in a study by Ou et al. [18]. The variation is noteworthy due to the established linear relationship between substrate CO_2 emission rate and temperature, as reported by Jung & Son [17]. Also, considering the relatively low airtightness of the bench test, exfiltration could have influenced the CO_2 emission rate measurements.

On the other hand, in the full-scale experiment FS-OL-44%, there was a notable correlation between the CO_2 emission rate and temperature. This aligns with prior research that has demonstrated a linear rise in the CO_2 emission rate of fructification substrate with increasing temperature [11,13]. The full-scale experiment yielded higher rates, with a rate of 37.76 μg $CO_2 \cdot s^{-1} \cdot kg_{sub}^{-1}$ at 21 °C. This difference can likely be attributed to the substantial proportion of oyster mushroom substrates, accounting for 44% of the total in

the FS-OL-44% experiment. Oyster substrate releases a larger quantity of emitted CO_2 compared to shiitake strains [12]. By comparison, an experiment by Hyunja Chung [8] with oyster mushrooms on wood substrate during incubation yielded an average release of 53.5 μg $CO_2 \cdot s^{-1} \cdot kg_{sub}{}^{-1}$.

These results distinctly demonstrated the temperature-dependent nature of CO_2 emission rates for shiitake and oyster mushroom substrates. Notably, oyster substrates exhibited a significantly higher CO_2 emission rate, which was twice as high during the incubation and even higher during fructification, compared to shiitake substrates. This suggests that fewer oyster mushrooms would be required compared to shiitake mushrooms to establish a CO_2 equilibrium for the synergistic cultivation of mushrooms and leafy greens. Future studies should include a diverse array of oyster strains, indoor environmental conditions, and different substrate types. Such comprehensive research is crucial for identifying the most suitable combination for CO_2 exchange synergies in plant cultivation.

4.2. Heat Exchange Rate

During the incubation experiments, SS-CL-53%, a low heat exchange rate was observed from the shiitake substrate with an average heat exchange rate of 4.2 ± 2.9 W for a substrate mass of 215 kg. It is essential to highlight the only point of comparison for the heat exchange rate is for the study on oyster mycelium grown on a straw substrate, which reported a rate of 7.08 $W \cdot kg^{-1}$ [15]. This discrepancy can be attributed to the slower metabolism of shiitake strains and their carbon-rich substrate mix [12,20], resulting in lower exothermic reactions compared to strains like oyster mushrooms grown on straw.

The low heat exchange rate observed in the shiitake substrate suggests a reduced need for air cooling, which can be advantageous when considering potential synergies between mushroom and leafy green farms. The cultivation of leafy greens in controlled environments requires constant cooling [13]. In installations where heating is needed more frequently than cooling throughout the year, oyster strains may be preferred over shiitake strains from an energy efficiency standpoint as they release more heat. Moreover, selecting a specific mushroom genus based on seasonal weather conditions could present an energy efficiency opportunity when cultivated in synergy with greenhouses. Heat-generating mushroom species could be prioritized during the colder months, aligning with greenhouse heating requirements, while opting for mushroom species with a lower heat exchange rate during the warmer months when cooling becomes essential.

5. Conclusions

In this study, CO_2 emission and heat exchange rates for shiitake and oyster mushrooms from the literature were supplemented with experimental data gathered through three different experiments using two other testing spaces. The results revealed that at an indoor temperature of 21 °C, shiitake, oyster, and mixed substrates exhibited average CO_2 emission rates of 24.9, 53.5, and 37.7 μg $CO_2 \cdot s^{-1} \cdot kg_{sub}{}^{-1}$, respectively. During fructification at 24 °C, these rates are 26.7 and 150.8 7 μg $CO_2 \cdot s^{-1} \cdot kg_{sub}{}^{-1}$ for shiitake and oyster, respectively. The heat exchange rates during incubation are 0.02 and 7.08 $W \cdot kg_{sub}{}^{-1}$ for shiitake and oyster substrates, respectively. These rates play a crucial role in conducting feasibility analyses on the potential of using the return air from mushroom farms to enrich the air of leafy green farms. As the world moves towards more sustainable and interconnected farming practices, harnessing the CO_2 and heat exchange potential of various mushroom strains could play a pivotal role. This study serves as a foundation for further exploration in this direction.

Author Contributions: Conceptualization, methodology, investigation, and writing—review and editing, M.-A.M., D.M. and D.B.; original idea, formal analysis and data curation, M.-A.M.; supervision, D.M. and D.B. All authors have read and agreed to the published version of the manuscript.

Funding: This research was supported by NSERC research grants RGPIN-2014-04971 and RGPIN-2020-04576.

Institutional Review Board Statement: Not applicable.

Informed Consent Statement: Not applicable.

Data Availability Statement: Most data are contained within the article.

Conflicts of Interest: The authors declare no conflict of interest.

References

1. Chang, S.T.; Miles, P.G. *Mushrooms: Cultivation, Nutritional Value, Medicinal Effect, and Environmental Impact: Second Edition*; CRC Press: Boca Raton, FL, USA, 2004.
2. Zhang, Y.; Geng, W.; Shen, Y.; Wang, Y.; Dai, Y.C. Edible mushroom cultivation for food security and rural development in China: Bio-innovation, technological dissemination and marketing. *Sustainability* **2014**, *6*, 2961–2973. [CrossRef]
3. Mahamad, K.; Mansuriwong, P.; Petlamul, W. Application of Smart Farm System to Enhance Phoenix Oyster Mushroom Production. *ASEAN J. Sci. Technol. Rep.* **2021**, *24*, 47–57. [CrossRef]
4. Kassim, M.R.M.; Mat, I.; Yusoff, I.M. Applications of internet of things in mushroom farm management. In Proceedings of the 2019 13th International Conference on Sensing Technology (ICST), Sydney, NSW, Australia, 2–4 December 2019; pp. 5–10. [CrossRef]
5. Cadavid, H.; Garzón, W.; Pérez, A.; López, G.; Mendivelso, C.; Ramírez, C. Towards a Smart Farming Platform: From IoT-Based Crop Sensing to Data Analytics. In *Advances in Computing*; Springer: Cham, Switzerland, 2018; pp. 237–251.
6. De-Pablos-Heredero, C.; Montes-Botella, J.L.; García-Martínez, A. Sustainability in smart farms: Its impact on performance. *Sustainability* **2018**, *10*, 1713. [CrossRef]
7. Jung, D.H.; Son, J.E. CO_2 utilization strategy for sustainable cultivation of mushrooms and lettuces. *Sustainability* **2021**, *13*, 5434. [CrossRef]
8. Chung, J.H. Carbon Dioxide Generation by Fungal Mycelium during Spawn Run. Master's Thesis, The University of Arizona, Tucson, AZ, USA, 2021.
9. Li, Y.; Ding, Y.; Li, D.; Miao, Z. Automatic carbon dioxide enrichment strategies in the greenhouse: A review. *Biosyst. Eng.* **2018**, *171*, 101–119. [CrossRef]
10. Kitaya, Y.; Tani, A.; Kiyota, M.; Aiga, I. Plant growth and gas balance in a plant and mushroom cultivation system. *Adv. Sp. Res.* **1994**, *14*, 281–284. [CrossRef] [PubMed]
11. Jung, D.H.; Kim, C.K.; Oh, K.H.; Lee, D.H.; Kim, M.; Shin, J.H.; Son, J.E. Analyses of CO_2 concentration and balance in a closed production system for king oyster mushroom and lettuce. *Hortic. Sci. Technol.* **2014**, *32*, 628–635. [CrossRef]
12. Stamets, P. *Growing Gourmet and Medicinal Mushrooms*, 2nd ed.; Ten Speed Press: Berkeley, CA, USA, 2000.
13. Talbot, M.H.; Monfet, D. Estimating the impact of crops on peak loads of a Building-Integrated Agriculture space. *Sci. Technol. Built Environ.* **2020**, *26*, 1448–1460. [CrossRef]
14. Cotter, T. *Organic Mushroom Farming and Mycoremediation*; Chelsea Green Publishing: Chelsea, VT, USA, 2014.
15. Koncsag, C.I.; Kirwan, K. Heat and Mass Transfer Study during Wheat Straw Solid Substrate Fermentation with P. ostreatus. *Chem. Bull. Politeh. Univ. Timis.* **2010**, *55*, 1–4.
16. Chanter, D.O.; Thornley, J.H.M. Mycelial Growth and the Initiation and Growth of Sporophores in the Mushroom Crop: A Mathematical Model. *J. Gen. Microbiol.* **1978**, *106*, 55–65. [CrossRef]
17. Jung, D.H.; Son, J.E. Carbon Dioxide Emission Modeling of King Oyster Mushroom before and after Thinning Processes According to Temperature and Growth Stage. *J. Bio-Environ. Control* **2021**, *30*, 140–148. [CrossRef]
18. Ou, Y.; Zhang, L.; Yu, H.; Song, C.; Zhang, M.; Tan, Q.; Shang, X. CO_2 release from Lentinula edodes strains under different cultivation modes. *Acta Edulis Fungi* **2020**, *27*, 37–44.
19. Jung, D.H. CO_2 Control Strategies for Sustainable Cultivation of King Oyster Mushrooms and Romaine Lettuces in a Closed Production System. Master's Thesis, Seoul National University, Seoul, Republic of Korea, 2016.
20. ASHRAE. *ASHRAE Fundamentals (SI)*; ASHRAE: Peachtree Corners, GA, USA, 2017.
21. Matsumoto, M.; Nishimura, T. Mersenne Twister: A 623-Dimensionally Equidistributed Uniform Pseudo-Random Number Generator. *ACM Trans. Model. Comput. Simul.* **1998**, *8*, 3–30. [CrossRef]
22. Kandasamy, P.; Moitra, R.; Mukherjee, S. Measurement and Modeling of Respiration Rate of Tomato (Cultivar Roma) for Modified Atmosphere Storage. *Recent Pat. Food. Nutr. Agric.* **2015**, *7*, 62–69. [CrossRef] [PubMed]

Disclaimer/Publisher's Note: The statements, opinions and data contained in all publications are solely those of the individual author(s) and contributor(s) and not of MDPI and/or the editor(s). MDPI and/or the editor(s) disclaim responsibility for any injury to people or property resulting from any ideas, methods, instructions or products referred to in the content.